ELSEVIER

Journal of Biomechanics 32 (1999) 1091–1097

JOURNAL OF BIOMECHANICS

www.elsevier.com/locate/jbiomech

Glenoid cancellous bone strength and modulus

Carolyn Anglin[a,b,*], Patricia Tolhurst[a], Urs P. Wyss[a,b], David R. Pichora[a]

[a]*Clinical Mechanics Group, Queen's University, Kingston, Canada*
[b]*Sulzer Orthopedics Ltd., Winterthur, Switzerland*

Received 6 May 1997; accepted 18 April 1999

Abstract

The objectives of this study were to determine the strength and modulus of glenoid cancellous bone, including regional variations. The motivations were: to select a suitable bone substitute for standardized testing of glenoid prosthesis loosening, to assist in shoulder prosthesis design and to provide input data for finite element analyses. Ten glenoids from eight cadavers (mean age, 81) were tested by in situ indentation. Mean strength ranged from 6.7 to 17 MPa for the ten glenoids, the overall mean being 10.3 MPa. Mean E moduli ranged from 67 to 171 MPa for the individual glenoids, the overall mean being 99 MPa. These values are likely at the lower end of what would be expected for normal bone since strength and modulus decrease with age and the available specimens were older. These values may be appropriate for prosthesis design, however, since mechanical properties are reduced in rheumatoid arthritic bone. Regional trends were very similar for modulus and strength. The strongest region was postero-superior. The central column, correlating with the keel position in many glenoid components, was weaker than both the anterior and posterior regions but deeper. A large drop in strength and modulus below the subchondral layer emphasizes the importance of maintaining this layer during prosthetic replacement.

Keywords: Shoulder; Glenoid; Bone; Mechanical properties; Total shoulder arthroplasty

1. Introduction

Mechanical properties of bone are of interest in prosthesis design for several reasons. The absolute values of strength and modulus can be used in artificial bone models and finite element analyses to evaluate alternative designs. Relative variations, both in cross-section and in depth, may suggest the best placement for fixation or a preferred surgical technique. Variations from one glenoid to another guide the range of shapes and sizes required. Although the study goals were broader, the investigation was motivated by the need to choose a glenoid bone substitute for experimental testing; a range of polyurethane foam bone substitutes was available with specified densities, moduli and strengths (Last-a-Foam, General Plastics, Tacoma, WA).

Whereas the mechanical properties of cortical bone are relatively consistent among sites, the properties of cancellous bone vary greatly (Cowin, 1989; Martens et al., 1983; Goldstein, 1987; Linde, 1994). Many studies have investigated the properties of femoral and tibial cancellous bone, but information on glenoid cancellous bone properties is limited, particularly with respect to strength and depth (see Table 1). Poor bone quality is an important contributor to glenoid component loosening, loosening being the most common clinical complication in total shoulder arthroplasty (Wirth and Rockwood, 1996).

2. Methods and materials

The mechanical bone properties were derived in situ with a 2.95 mm flat cylindrical indentor attached to an Instron 1122 testing machine. Indentation of the intact glenoid, as opposed to testing extracted cubes or cylinders, maintained the structure of the glenoid and allowed the strength and modulus to be investigated throughout the glenoid vault. Ten embalmed glenoids were tested including two right–left pairs. Embalming only increases the modulus of cancellous bone by a few percent (Hodgkinson and Currey, 1990; Linde, 1994), insignificant in comparison to the variations among individuals.

* Corresponding author. Sulzer Orthopedics Ltd., P.O. Box 65, CH-8404 Winterthur, Switzerland. Tel.: + 41-52-262-68-32; fax: + 41-52-262-01-87.

E-mail address: carolyn.anglin@sulzer.ch (C. Anglin)

0021-9290/99/$ - see front matter
PII: S0021-9290(99)00087-1

Table 1
Glenoid properties in the literature

Study and method	Mean properties[a]	Number and age	Regional variations
Mansat et al. (1998); Baréa (1998); Baréa et al. (1997): Ultrasound, CT; cubes	E_1[b] = 372 MPa E_2[b] = 222 MPa E_3[b] = 198 MPa $\rho = 0.27$ g/cm^3	6 spec. (3 pairs); 80 ± 9 yr	Central and posterior moduli; highest inferior weaker; decrease with depth; anisotropic
Frich et al. (1997,1998); Frich and Odgaard (1995); Frich (1994): CT, MRI; (a) penetrometer, (b) cylinders (central) and (c) cubes (sup. and inf.)	σ_a[c] = 37 MPa $E_b = 105$ MPa $E_c = 411$ MPa $\rho_b = 0.34$ g/cm^3 $\rho_c = 0.38$ g/cm^3 $v_c = 0.26$	20 healthy spec. (10 pairs); 31–74 yr (mean 57); 6 rheum. arthritic (RA) spec.; 45–75 yr (mean 56)	Postero-superior strongest; posterior > anterior; anisotropic close to surface, isotropic deeper; RA bone volume fractions half that of healthy
Batte et al. (1996); Batte (1996): CT, indentation; slices	K[d] ≈ 370 MPa ρ = high volume fraction of bone	8 spec (0 pairs); 55–74 yr, plus one in early 40s	Superior stiffest; ant.-post. trends varied; weaker below 6 mm
Mason et al. (1994): CT	$\rho = 0.37$ g/cm^3	16 spec. (6 pairs); age not specified	Superior densest; central column weaker than post. or ant.; deepest portion inf. to antero-superior.
Müller-Gerbl et al. (1992): CT (in vivo); (a) healthy, (b) gymnasts, (c) patient with dislocation	—	(a) 20 spec. yr (22–86) (b) 11 (16–29) (c) 1 (45)	Higher anterior and posterior density in young; more central in elderly

[a]E = modulus, ρ = density, σ = strength, v = Poisson's ratio, K = indentation modulus[d]
[b]E_1 is latero-medial, E_2 is antero-posterior, E_3 is supero–inferior
[c]penetrometer strength of 37 MPa ≈ 14 MPa ultimate strength (Hvid, 1988); taken at 2 mm below the surface
[d]indentation modulus, K, is the stress/strain from the indentor, which is higher than the elastic modulus

Table 2
Details of glenoid specimens

Glenoid	Age (yr)	Sex	Shoulder
1	96	F	R
2	70	F	L
3	62	F	L
4	See glenoid 3		R
5	92	M	L
6	See glenoid 5		R
7	79	F	L
8	82	M	R
9	70	F	L
10	93	F	L
Average	80.5	6F, 2M	6L,4R

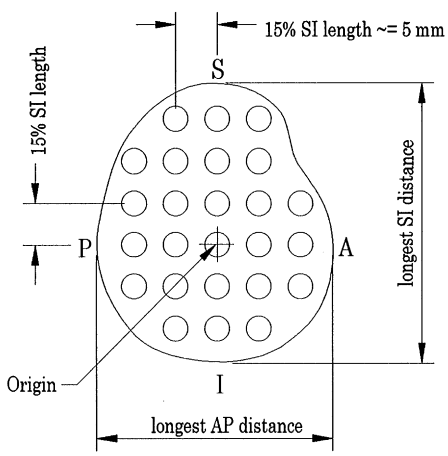

Fig. 1. Surface view of the glenoid. The five columns by six or seven rows were separated by 15% of the superior–inferior length (approximately 5 mm).

The average age of the specimens was 81 years and the majority were female (see Table 2). No specimens were visibly arthritic, i.e. a cartilage layer remained and there were no osteophytes or obvious erosion. No specimens were excluded.

The resected scapula was embedded in a hemi-cylindrical 5 cm radius mould of fibreglass resin. A grid was marked on the glenoid, with rows and columns spaced proportionally (Fig. 1), by 15% of the superior–inferior (SI) length (approximately 5 mm). This ensured no effect between adjacent holes (Little et al., 1986). The origin was defined as the intersection of the longest and widest dimensions (corresponding approximately to the 'bare area' identified by Frich, 1994 and by Warner et al., 1998).

Table 3
Glenoid dimensions[a]

Glenoid no.	SI Length (mm)	AP Length (mm)	Sup. Portion (%)	Ant. Portion (%)
1	30.0	24.0	57	48
2	31.0	25.0	50	52
3	30.0	22.0	60	45
4	30.0	22.0	58	52
5	33.0	27.0	67	54
6	32.5	22.0	71	50
7	30.0	23.0	72	52
8	34.0	25.0	65	54
9	30.5	28.0	61	52
10	35.0	27.0	56	48
Average	31.6	24.5	61.7	50.7

[a]origin = intersection of longest and widest dimensions (see Fig. 1).

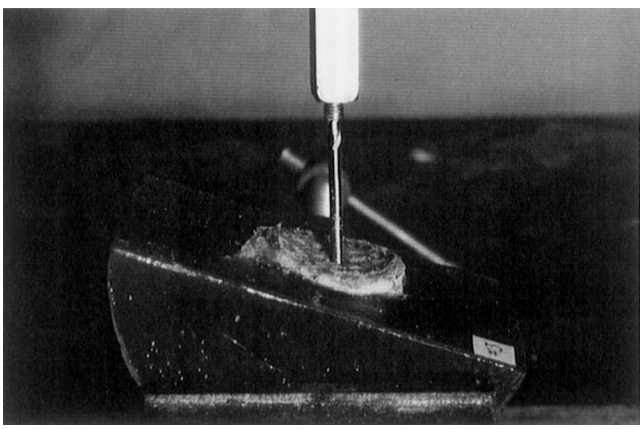

Fig. 2. Experimental setup for the bone indentation. The hemi-cylindrical resin mould could be rotated in the vise such that the indentor was normal to the glenoid surface along the central superior–inferior axis.

The SI axis was almost 30% longer, on average, than the anterior–posterior (AP) axis with the anterior, posterior and inferior portions being roughly equal, suggesting a pear shape (Table 3).

After removal of the cartilage, the gridpoints were flattened with a 3.1 mm flat-end milling cutter allowing clearance for the indentor. The subchondral layer was tested but not included in the cancellous results.

The hemi-cylinder, having the flat ends parallel to the SI axis, could be rotated to any angle in a vise (Fig. 2). The 3 mm indentor was directed radially, visually normal to the surface of the central SI column, as seen in Fig. 3. This mimicked the direction of load normally applied by the humeral head. No adjustment was made for the smaller anterior–posterior curvature as this would have required a different orientation for each hole with little gain.

For each layer, indentation was performed at 2 mm/min, continuing until a sudden reduction in force indicated bone failure, or to a maximum distance of

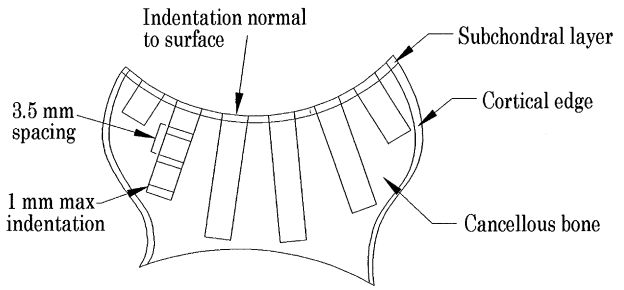

Fig. 3. Cross-sectional view of the glenoid. The indentation sequence was: 1. Mill a 3.1 mm flat hole normal to the surface at the defined grid points. 2. Indent each hole with a 2.95 mm indentor, recording the indentor load and displacement. 3. Mill each hole 3.5 mm deeper from the original surface. 4. Repeat the indentation sequence until reaching the cortical edge or a maximum 31.5 mm. 5. Remove the non-cancellous sites from the data after slicing the tested glenoid.

1 mm. After the completion of a layer, the holes were milled a further 3.5 mm from the surface ensuring that the following layer was unaffected (Katoh et al., 1996). Tests were conducted up to 31.5 mm or until the cortical edge was reached. After completion of the testing, the glenoid was sliced in the SI direction through each column of holes in order to establish which sites were cancellous (Fig. 3). Any test sites within 2 mm of the cortical edge were removed from the data for calculations; since this included the holes that had reached the 1 mm depth before failure, no data needed to be censored in the statistical analysis.

The data were fit to a Weibull distribution, often used to characterize strength data (Bury, 1975). The logarithms of the regional data were first compared using an analysis of variance (ANOVA) with $\alpha = 0.05$. If significant differences were found, regions were compared using the least significant difference method (Montgomery, 1997) with $\alpha = 0.05$. The matched glenoids were compared hole by hole, using paired t-tests.

In engineering terms and for the purposes of the bone substitute, a material has failed whether it yields or breaks. Thus, if flattening of the curve indicating substantial plastic deformation occurred before ultimate failure, the failure strength was calculated from the yield load; otherwise the ultimate load was used. Substantial plastic deformation corresponded to at least 0.1 mm. The rationale for not always using the ultimate load was that bone fails in two different modes. Failure by yielding is related to transverse bending of trabeculae whereas failure showing a peak load is related to axial buckling or brittle fracture of trabeculae (Gibson, 1985).

Strength was calculated as the failure load divided by the area of the indentor. The modulus was calculated using the traditional equation for indentation (Timoshenko and Goodier, 1970) as:

$$\left[E = \frac{(1 - v^2)}{2r} \cdot \frac{P}{\delta} \right] \quad (1)$$

Table 4
Glenoid cancellous strength and modulus

Glen.	Failure strength (MPa)			Elastic modulus (MPa)		
	Mean[a]	S.D.	Range	Mean[a]	S.D.	Range
1	7.5	± 6.2	0.3–24	67	± 63	0.1–281
2	9.4	± 8.8	0.9–49	69	± 54	0.1–377
3	(17.2)	(± 10.0)	4.8–50	(128)	(± 74)	4.4–303
4	16.9	± 11.0	4.0–69	171	± 89	33–470
5	(6.7)	(± 5.0)	0.4–33	(74)	(± 51)	0.2–194
6	7.4	± 5.3	0.6–24	82	± 57	2.1–238
7	9.7	± 8.0	1.5–41	101	± 72	10–319
8	12.6	± 10.3	1.2–53	112	± 87	2.6–382
9	9.7	± 10.0	0.8–73	91	± 72	7.2–423
10	8.9	± 5.6	1.5–28	98	± 59	23–289
All[b]	10.3	± 3.1	0.3–73	99	± 33	0.1–470

[a]All cancellous data were included, therefore the mean is the average over all depths and regions.
[b]Glenoids 3 and 5 were not included in the calculation of the overall means because they were paired with glenoids 2 and 4, respectively.

where v is the Poisson's ratio, $2r$ is the diameter of the indentor and P/δ is the slope of the load versus displacement curve. The slope was taken as the most linear portion of the curve prior to yielding. This equation does assume continuous, homogeneous, isotropic conditions, however these assumptions are common in macroscopic testing of cancellous bone. Poisson's ratio was chosen to be 0.25 as an average value in the literature (Keaveny et al., 1993; Linde, 1994), and agrees with that found by Frich and coworkers (1997) for the glenoid. Even though there is uncertainty in the value of the Poisson's ratio a value of 0.2 as opposed to 0.25, for example, would only increase the calculated modulus by 2.4%. The recorded deformation included the deformation of the glenoid bone, the testing machine and the supporting resin. The slope was corrected for machine stiffness, resulting in a mean 3% increase in modulus. The resin had a similarly small effect.

Mean glenoid depth was calculated by averaging the maximum tested depth of each hole across the glenoids. If a hole location was outside an individual glenoid's surface it was given a depth of zero. Minimum glenoid depth was calculated as the shallowest depth tested.

3. Results

Mean strength ranged from 6.7 to 17.2 MPa for the individual glenoids; modulus ranged from 67 to 171 MPa (Table 4). The occasional very low modulus (five sites out of a total of 654) may have been due to not sufficiently removing the residual bone fragments following milling. When these five points were excluded, the fit to the Weibull distribution was excellent ($R^2 = 0.99$).

Pooled data include all locations and depths within a given region for all glenoids excluding the paired glenoids 3 and 5. Glenoids 3 and 5 were chosen from the two pairs so as to result in an equal number of right and left glenoids.

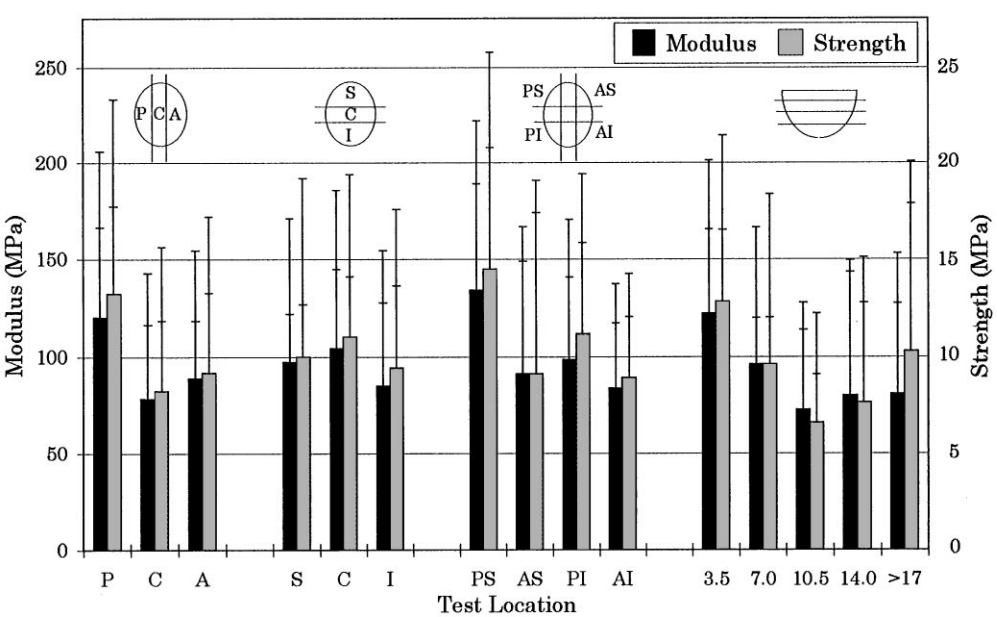

Fig. 4. Pooled modulus and strength by region. P, C, A = posterior region, central column and anterior region; S, C, I = superior region, central row and inferior region; PS, AS, PI, AI = postero-superior, antero-superior, postero-inferior and antero-inferior regions, all excluding central row and column; 3.5, etc. = depth in millimetres. The smaller standard deviation shows the variation across glenoids; the larger standard deviation indicates the variation for all indented positions. See Table 5 for significant differences.

Table 5
Glenoids showing significant differences[a]

Regions[b]	Strength	Modulus
P > A and P > C	7,9,10, Pooled	6,7,8,9
P > C and A > C	1,2,5,8	1,5,8
PS > AS,PI,AI	Pooled	Pooled
S,C,I	None	None
Depths: various[c]	All	All

[a]$p < 0.05$ using the LSD method following ANOVA (see Methods).
[b]See Fig. 4 for an explanation of the abbreviations.
[c]All glenoids had significant differences between some combinations of depth, but not always the same combinations.

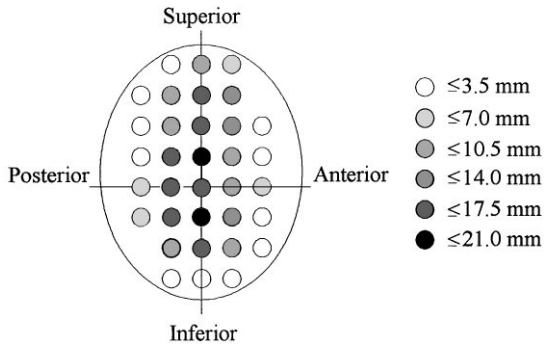

Fig. 5. Mean glenoid depth. This indicates the cancellous depth normally available for prosthetic fixation. Columns and rows were spaced approximately 5 mm apart. Although shown flat, the holes were directed radially.

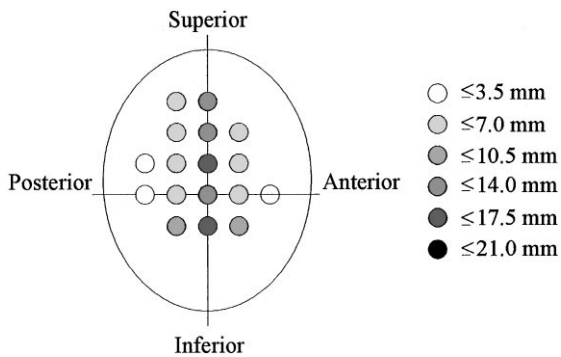

Fig. 6. Minimum glenoid depth. This implies a limit to prosthesis fixation depth.

Variations in strength and modulus by region showed almost identical patterns, based on the pooled data (Fig. 4). In both cases, the postero-superior region had the highest values. The posterior properties were much stronger than the anterior region and central column; in some cases the anterior region was also significantly stronger than the central column (Table 5). Trends in depth varied with each glenoid, but in the pooled data, strength and modulus decreased significantly over the first three layers. An even more marked decrease occurred between the subchondral layer (not included in the cancellous calculations) and the first cancellous layer. For example, the drop in pooled strength from the subchondral to the first cancellous layer was from 52 to 12 MPa; the corresponding drop in modulus was from 290 to 122 MPa. Strength, and especially modulus, increased again at even deeper layers causing a V-shaped pattern. Pair-wise treatment of the matched glenoids indicated a significant difference in modulus, but not in strength. There was a strong ($R^2 = 0.76$) linear relationship between strength (S) and elastic modulus (E), with $S = 0.10E$ for the pooled data. Relationships for individual glenoids varied from $S = 0.08E$ to $S = 0.13E$.

Sixteen percent of the indentations failed by yielding; the remainder reached a peak (ultimate) load without yielding. For those that yielded, the yield loads were $26 \pm 18\%$ less than their ultimate load. Although yielding occurred at all levels and regions, it tended to occur more at deeper levels.

The holes with the greatest mean depth (16–20 mm) and greatest minimum depth (11–14 mm) were located in the central superior-inferior column (Figs. 5 and 6), corresponding to the location of the keel in many glenoid prosthesis designs. In general, the inferior and antero-superior regions presented the greatest depths.

4. Discussion

Trends in the modulus and strength data were extremely similar. This strong linear relationship between strength and modulus is well supported in the literature (Linde et al., 1992; Martens et al., 1983).

Strength values were at the higher end of what has been reported at other sites, probably because most of those tests were done in unconfined compression (Keaveny and Hayes, 1993; Linde et al., 1992; Linde, 1994; Martens et al., 1983). Extraction of specimens leads to reduced strength and modulus due to the removal of trabecular cross-struts and surrounding material (Linde and Hvid, 1989). The only other strength values for the glenoid are from Frich and coworkers (1994,1997) using a penetrometer and are higher than in this study (Table 1).

Modulus values were lower than found by others for the glenoid (Batte et al., 1996; Mansat et al., 1998; Frich et al., superior–inferior cubes, 1997), although quite similar to Frich's (1997) central cylinders. This may be due to the lower density and older ages of our specimens, or may be due to differences in the loading conditions. Batte tested thin 3 mm glenoid slices with a 3 mm indentor, the calculated indentation modulus being higher than the traditional Young's modulus; Frich tested 7.5 mm high × 6.5 mm diameter cylinders and 7 mm cubes, reporting a large difference between the central cylinders

and the superior and inferior cubes; Mansat used an ultrasonic technique on 6 mm cubes, this technique often reporting higher values than for mechanical testing.

Since the radial direction is the strongest direction in the glenoid (Mansat et al., 1998; Frich et al., 1997,1998; see Table 1), the strength and modulus perpendicular to the radial direction would be lower than reported in the present study, the greatest difference being at the surface where the anisotropy is highest. All three directions can play a role in the resistance to eccentric loading of a glenoid prosthesis. The tendency towards more yielding failures at deeper levels connects two findings: that there is greater isotropy centrally (Frich et al., 1997) and that yielding occurs due to bending of trabeculae (Gibson, 1985). At the surface, the trabeculae are oriented perpendicular to the surface and usually result in ultimate failure due to buckling (Frich et al., 1998; Gibson, 1985). A more complete bone model for evaluating prosthesis performance should therefore include anisotropy.

A dramatic effect on bone properties has been shown with age (Ding et al., 1997; Keaveny and Hayes, 1993; McCalden et al., 1997; Weaver and Chalmers, 1966), showing up to an 80% decrease in modulus from age 20 to 80 due to changes in the trabecular density and architecture. Decreases in strength are less dramatic (Keaveny and Hayes, 1993). Our results are therefore appropriate only to an older population, however, this suits the shoulder arthroplasty population. Modulus and strength are lower in females than in males, over the age of 50 (Weavers and Chalmers, 1966). There is, however, a substantial degree of scatter in the age and sex data due to the activity level of the individual.

Rheumatoid arthritis (RA), a common indication in total shoulder arthroplasty, reduces glenoid density; according to Frich (1994) early RA demonstrated bone volume fractions half that of normal bone, i.e. 8–23% for RA as compared to 14–43% for normal glenoid bone. Since poor quality bone is a contributing factor to glenoid loosening (Frich et al., 1997; Wirth and Rockwood, 1996), a lower modulus and strength could be justified for mechanical testing and finite element analyses.

Our mean depth findings were similar to Mason and coworkers (1994) in that the greatest depth ran from postero-inferior to antero-superior. The transverse plane forms a narrow funnel whereas the coronal plane is wider, deeper and more square, as recently confirmed by Bicknell and coworkers (1998). There was a broad range of shapes, however, as evidenced by both Table 3 and Fig. 6, which presents a problem for deeper fixation of glenoid prosthetic components. In arthritic glenoids, the depth may be reduced even further (Boileau and Walch, 1999).

Posterior and anterior regions, particularly in the postero-superior region, appear to be more suitable for prosthetic fixation than the central region in terms of strength and modulus but the central column may be favoured due to depth. These findings are supported by Frich and coworkers (1997), Mason and coworkers (1994) and Devries (1995), whereas Mansat and coworkers (1998) suggest that the central and posterior regions are stiffer than the anterior. Stronger posterior properties are consistent with the normal functional use of the arm in front of the body (Frich et al., 1998).

A decrease in properties with depth as found in this study is typical (Aitken et al., 1985; Mansat et al., 1998; Batte et al., 1996; Harada et al., 1988; Frich et al., 1997), especially below the subchondral layer. This highlights the importance of maintaining the subchondral layer in prosthetic replacement, i.e. resecting as little bone as possible. It appears from Figs. 4 and 5 that the deepest regions were also the weakest. The data were reanalysed using depths only up to 10.5 mm in case this was a result of the pooling but the basic results were unchanged. As further confirmation, lower densities were often seen in the weaker regions on computed tomography scans.

High standard deviations for bone properties are common (Linde, 1994; Keaveny and Hayes, 1993; Martens et al., 1993; Goldstein et al., 1983). However, the small size of the indentor, spanning only a few trabecular spacings, caused even higher variability (Hvid, 1988). This is a trade off for greater resolution.

This study determined the strength and modulus throughout the cancellous glenoid vault of ten glenoids by means of in situ indentation testing. Mean strength was 10.3 MPa and mean modulus was 99 MPa with large variations within and among glenoids. Mean depth in the central column was 16–20 mm, decreasing quickly in the anterior and posterior directions. Shape varied considerably among the glenoids in terms of the length of the axes, the position of the origin and the distribution of depth. Deeper prosthesis fixation should be placed in the central column; shorter fixation should be placed in the stronger bone on the posterior and anterior sides.

Acknowledgements

The authors would like to thank Wayne Lyons of the Queen's University Anatomy department for the use of the glenoid specimens, Queen's University STATLAB for statistical assistance and Gerry Saunders and David Siu of the Clinical Mechanics Group at Queen's University for their technical assistance. Funding by Sulzer Orthopedics Ltd., Queen's Graduate School and the Ontario government is gratefully acknowledged.

References

Aitken, G.K., Bourne, R.B., Finlay, J.B., Rorabeck, C.H., Andreae, P.R., 1985. Indentation stiffness of the cancellous bone in the distal human tibia. Clinical Orthopaedics 201, 264–270.

Boileau, P., Walch, G., 1999. Normal and pathological anatomy of the glenoid: effects on the design, preparation, and fixation of the glenoid component. In: Walch, G., Boileau, (Eds.), Shoulder Arthroplasty. Springer, Berlin, pp. 127–140.

Baréa, C., 1998. Modélisation 3D par la méthode des éléments finis d'une articulation scapulo-humérale: application a l'étude des contraintes sur une épaule saine et avec différents types de glènes prothétiques. Ph.D. thesis, University of Paul Sabatier, Toulouse.

Baréa, C., Mansat, P., Hobatho, M.C., Darmana, R., Mansat, M., 1997. Mechanical properties of the glenoid cancellous bone. Transactions of the Orthopaedic Research Society 22, 877.

Batte, S.W.P., 1996. An evaluation of bone quality and implant stability in the glenoid: implications in prosthesis design. M.Sc. thesis, University of Western Ontario, London.

Batte, S.W.P., Cordy, M.E., Lee, T.Y., King, G.J.W., Johnson, J.A., Chess, D.G., 1996. Cancellous bone of the glenoid: correlation of quantitative CT and mechanical strength. Transactions of the Orthopaedic Research Society 21, 707.

Bicknell, R.T., Danter, M.R., Bennett, J., Patterson, S.D., King, G.J.W., Johnson, J.A., 1998. An anthropometric evaluation of the glenoid: implications in the design and fixation of a shoulder prosthesis. Transactions of the Orthopaedic Research Society 23, 270.

Bury, K.V., 1975. In: Statistical Models in Applied Science. Wiley, New York.

Cowin, S.C., 1989. Bone Mechanics. In: CRC Press Inc.. Boca Raton, FL.

DeVries, S., 1995. A three-dimensional finite element analysis of the glenoid with and without a total shoulder arthroplasty component. M.Sc. thesis, Queen's University, Kingston.

Ding, M., Dalstra, M., Danielsen, C.C., Kabel, J., Hvid, I., Linde, F., 1997. Age variations in the properties of human tibial trabecular bone. Journal of Bone and Joint Surgery [British] 79B (6), 995–1002.

Frich, L.H., 1994. Glenoidal knoglestyrke og koglestruktur. Thesis, University Hospital Aarhus, Aarhus.

Frich, L.H., Jensen, N.C., Odgaard, A., Pedersen, C.M., Søjbjerg, J.O., Dalstra, M., 1997. Bone strength and material properties of the glenoid. Journal of Shoulder and Elbow Surgery 6 (2), 97–104.

Frich, L.H., Odgaard, A., 1995. Bone architecture of the normal and rheumatoid arthritic glenoid. Transactions of the Orthopaedic Research Society 20, 683.

Frich, L.H., Odgaard, A., Dalstra, M., 1998. Glenoid bone architecture. Journal of Shoulder and Elbow Surgery 7 (4), 356–361.

Gibson, L.J., 1985. The mechanical behaviour of cancellous bone. Journal of Biomechanics 18 (5), 317–328.

Goldstein, S.A., 1987. The mechanical properties of trabecular bone: dependence on anatomic location and function. Journal of Biomechanics 20 (11/12), 1055–1061.

Goldstein, S.A., Wilson, D.L., Sonstegad, D.A., Matthews, L.S., 1983. The mechanical properties of human tibial trabecular bone as a function of metaphyseal location. Journal of Biomechanics 16 (12), 965–969.

Harada, Y., Wevers, H.W., Cooke, T.D.V., 1988. Distribution of bone strength in the proximal tibia. Journal of Arthroplasty 3 (2), 167–175.

Hodgskinson, R., Currey, J.D., 1990. The effect of variation in structure on the Young's modulus of cancellous bone: a comparison of human and non-human material. Proceedings of the Institution of Mechanical Engineers [H] 204, 115–121.

Hvid, I., 1988. Trabecular bone strength at the knee. Clinical Orthopaedics 227, 210–221.

Katoh, T., Griffin, M.P., Wevers, H.W., Rudan, J., 1996. Bone hardness testing in the trabecular bone of the human patella. Journal of Arthroplasty 11 (4), 460–468.

Keaveny, T.M., Hayes, W.C., 1993. A 20-year perspective on the mechanical properties of trabecular bone. Journal of Biomechanical Engineerings 115, 534–542.

Linde, F., 1994. Elastic and viscoelastic properties of trabecular bone by a compression testing approach. Danish Medical Bullelin 41 (2), 119–138.

Linde, F., Hvid, I., 1989. The effect of constraint on the mechanical behaviour of trabecular bone specimens. Journal of Biomechanics 22 (5), 485–490.

Linde, F., Hvid, I., Madsen, F., 1992. The effect of specimen geometry on the mechanical behaviour of trabecular bone specimens. Journal of Biomechanics 25 (4), 359–368.

Little, R.B., Wevers, H.W., Siu, D., Cooke, T.D.V., 1986. A three-dimensional finite element analysis of the upper tibia. Journal of Biomechanical Engineering 108, 111–119.

Mansat, P., Baréa, C., Hobatho, M.C., Darmana, R., Mansat, M., 1998. Anatomic variation of the mechanical properties of the glenoid. Journal of Shoulder Elbow Surgery 7 (2), 109–115.

Martens, M., Van Audekercke, R., Delport, P., De Meester, P., Mulier, J.C., 1983. The mechanical characteristics of cancellous bone at the upper femoral region. Journal of Biomechanics 16 (12), 971–983.

Mason, M.D., Kalus, R.M., Thornhill, T.S., Cheal, E.J., 1994. Examination of the bone density and geometry of the glenoid vault: influence on component design. Transactions of the Orthopaedic Research Society 19, 830.

McCalden, R.W., McGeough, J.A., Court-Brown, C.M., 1997. Age-related changes in the compressive strength of cancellous bone. Journal of Bone and Joint Surgery [American] 79A (3), 421–427.

Montgomery, D.C., 1997. Design and Analysis of Experiments. 4th Edition. Wiley, New York.

Müller-Gerbl, M., Putz, R., Kenn, R., 1992. Demonstration of subchondral bone density patterns by three-dimensional CT osteoabsorptiometry as a noninvasive method for in vivo assessment of individual long-term stresses in joints. Journal of Bone Mineral Research 7 (Suppl. 2), S411–S418.

Timoshenko, S.P., Goodier, J.N., 1970. Theory of Elasticity. 3rd Edition. McGraw-Hill, New York, pp. 408.

Warner, J.J.P., Bowen, M.K., Deng, X., Hannafin, J.A., Arnoczky, S.P., Warren, R.F., 1998. Articular contact patterns of the normal glenohumeral joint. Journal of Shoulder and Elbow Surgery 7 (4), 381–388.

Weaver, J.K., Chalmers, J., 1966. Cancellous bone: its strength and changes with aging and an evaluation of some methods for measuring its mineral content. Journal of Bone and Joint Surgery [American] 48A (2), 289–298.

Wirth, M.A., Rockwood, C.A.J., 1996. Current concepts review: complications of total shoulder-replacement arthroplasty. Journal of Bone and Joint Surgery [American] 78A (4), 603–616.